Electronic Supplementary Material (ESI) for Catalysis Science & Technology.
This journal is © The Royal Society of Chemistry 2023

Supporting Information

Catalyst characterization

Phase measurement was carried out on a X-ray diffractometer (XRD) **(**Rigaku D/MAX 2200PC) using Ni-filtered Cu Kα radiation at 40 kV and 30 mA. Phase evolution during the OPDH-CO_2 reaction was observed on a Rigaku Smart Lab diffractometer attached an *in situ* cell. Sample of 50 mg was placed into the cell and pretreated at 550 °C for 1 h in a N_2 flow (10 mL·min^{-1}). Then, a C_3H_8-CO_2 (1:1) flow (20 mL·min^{-1}) was switched into and the spectra were recorded each 30 min during the processive 160 min with scanning speed of 0.1 s and step width of 0.01º.

Micro morphology was observed on a field emission scanning electron microscope (FESEM) (Czech TESCAN MIRA LMS) at 30 kV and a transmission electron microscope (TEM) (FEI Talos F200X) at 200 kV.

Texture parameters were measured on a surface analysis instrument **(**JW-BK132F) using N_2 physicoadsorption. Sample of 200 mg was degassed at 250 °C for 4 h prior to measurement. The specific surface area was obtained using the Brunauer-Emmett-Teller(BET) model. Pore volume and distribution were obtained using the Barrett-Joyner-Halenda (BJH) model.

CO_2/C_3H_8 temperature-programmed desorption (CO_2/C_3H_8-TPD) was carried out on a chemisorption instrument (Micromeritics AutoChem II 2920). Sample of 50 mg was placed into a U-shaped quartz tube and pretreated at 350 °C for 1 h in a He flow (30 mL·min^{-1}). Then the sample was cooled down to 50 °C and adsorbed CO_2/C_3H_8 (30 mL·min^{-1}) for 30 min. Next, the sample was purged by the He flow for 1 h. Subsequently, as the temperature rose to 800 °C at a rate of 10 °C·min^{-1} the desorption of CO_2 was recorded using TCD. For *H_2 temperature-programmed reduction* (H_2-TPR), sample of 50 mg was loaded into the quartz tube followed by pretreatment at 300 °C for 1 h, and cooled down to ambient temperature in the He flow. Then, the H_2 consumed was recorded in a 10% H_2/Ar flow (30 mL·min^{-1}) as the temperature rose to 800 °C at 10 °C·min^{-1}.

Surface element valence analysis was performed using X-ray photoelectron spectroscopy (XPS) (Thermo Scientific K-Alpha spectrometer) using Al Kα X-ray radiation source. The base pressure of the chamber was less than 5×10^{-8} Pa. The binding energy (B.E.) was calibrated to adventitious carbon using the C1s peak at 284.8 eV.

NH_3 temperature-programmed desorption (NH_3-TPD) was performed on a TP-5080 adsorption instrument. Sample of 50 mg was pretreated in a He flow (30 mL·min^{-1}) at 550 °C for 1 h and then cooled down to ambient temperature. Then NH_3 was adsorbed at 100 °C for 30 min followed by purge in the He flow for 0.5 h. The desorption of NH_3 was recorded using TCD as the temperature was raised from ambient temperature to 600 °C at 10 °C·min^{-1}.

Thermogravimetric (TG) analysis of the used catalyst samples was carried out on a thermogravimetric analyzer (NETZSCH STA 449). Sample of 20 mg was heated from ambient temperature to 800 °C at a rate of 20 °C·min^{-1} in an air flow (30 mL·min^{-1}) and the weight was synchronously recorded.

Raman spectra were recoreded on a HORIBA Scientific LabRAM HR Evolution spectrophotometer equipped with a solid state laser (532 nm wave-length, 17 mW capacity) as the excitation source and a 5x objective lens. Spectra were collected at ambient temperature in the wave number range of 100−2000 cm^{-1}.

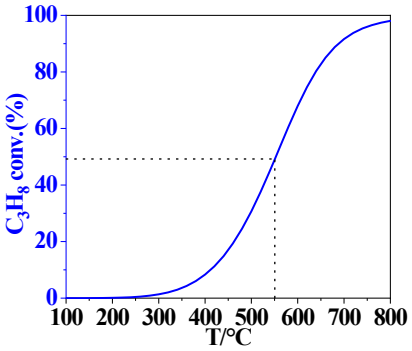

Fig. S1 Equilibrium conversions of OPDH-CO_2 reaction.
CO_2/C_3H_8=1, 0.1 MPa.

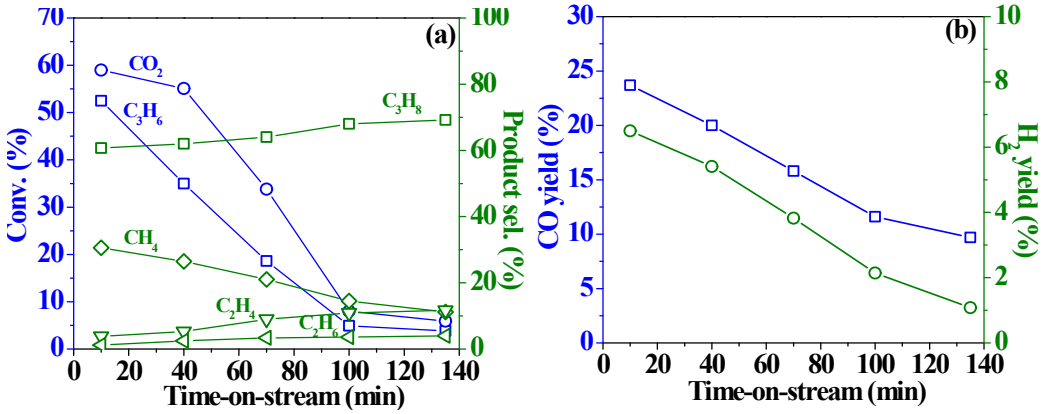

Fig. S2 C_3H_6 reaction with CO_2 on Fe_2O_3-3ZrO_2.
C_3H_6 (CO_2) conv. and product sel. (a); CO (H_2) yield (b)
$C_3H_6/CO_2/Ar$=1/1/1.5, W/F=12.5 g·h·mol^{-1}, 550 °C and 0.1 MPa.

Table S1 Reported catalytic activity for OPDH-CO_2

Cats	T (°C)	$n(CO_2)/n(C_3H_8)$	WHSV/ g_{C3H8} $g_{cat}^{-1}h^{-1}$	C_3H_8 conv. (%)	CO_2 conv. (%)	C_3H_6 sel. (%)	STY/ mol_{C3H6} $kg_{cat}^{-1}h^{-1}$	Ref.
$Cr_{2.0}$SiBeta	550	5	1.2	24.8	4.0	87.1	6.2	1
Cr-O/Al_2O_3	550	5	1.2	12.9	-	88.3	3.3	2
Cr_2O_3-ZrO_2	550	2	0.3	51.1	-	81.7	2.9	3
CrO_x/SBA-15	550	2	0.3	24.2	-	83.9	1.5	4
CrO_x/SiO_2	600	4	1.2	70	15.3	79	15.8	5
Ga_2O_3-Al_2O_3	500	2	0.15	49.7	-	91.7	1.6	6
Ga_2O_3-ZSM-48	600	2	0.3	52.6	-	42.2	1.6	7
In_2O_3-Al_2O_3	600	4	0.15	35	10.0	75	0.9	8
In_2O_3/Al_2O_3	600	4	0.15	14	11.0	80	0.4	9
V-MCM-41	600	4	1.0	58	10.5	90	12.4	10
V_2O_5-Cr_2O_3	550	1/3	3.5	9.9	5.0	95.9	7.9	11
V_2O_5-MoO_3	550	1/3	3.5	10.1	3.3	96.0	8.1	11
Fe_3Ni_1/CeO_2	550	1	11.8	2.7	4.0	58.2	3.9	12
5FeCeO_2	550	1	0.59	9.50	11.0	39.0	0.5	13
Fe_2O_3-3ZrO_2	550	1	1.1	39.9	28.2	83.7	8.7	this work

T---reaction temperature; STY---space time yield. STY--- calculated using the literatrue data.

References

1 P. Michorczyk, K. Zeńczak-Tomera, B. Michorczyk, A. Węgrzyniaka, M. Bastaa, Y. Millotb, L. Valentinb and S. Dzwigajb, *J CO_2 Utiliz.*, 2020, **36**, 54–63.

2 P. Michorczyk, K. Zeńczak, R. Niekurzak and J. Ogonowski, *Polish J Chem. Technol*., 2012, **14**, 77−82.

3 R. Wu, P. Xie, Y. Cheng, Y. Yue, S. Gu, W. Yang, C. Miao, W. Hua and Z. Gao, *Catal. Commun*., 2013, **39**, 20–23.

4 X. Zhang, Y. Yue and Z. Gao, *Catal. Lett*., 2002, **83**, 19–25.

5 H. M. Wang, Y. Chen, X. Yan, W. Z. Lang and Y. J. Guo, *Microporous Mesoporous Mater*., 2019, **284**, 69–77.

6 M. Chen, J. Xu, Y. M. Liu, Y. Cao, H. Y. He, J. H. Zhuang and K. N. Fan, *Catal. Lett*., 2008, **124**, 369–375.

7 Y. Ren, J. Wang, W. Hua, Y. Yue and Z. Gao, *J. Ind. Eng. Chem*., 2012, **18**, 731–736.

8 M. Chen, J. Xu, Y. Cao, H. Y. He, K. N. Fan and J. H. Zhuang, *J. Catal*., 2010, **272**, 101–108.

9 M. Chen, J. L. Wu, Y. M. Liu, Y. Cao, L. Guo, H. Y. He and K. N. Fan, *Appl. Catal., A*, 2011, **407**, 20–28

10 Z. F. Han, X. L. Xue, J. M. Wu, W. Z. Lang and Y. J. Guo, *Chin. J. Catal*., 2018, **39**, 1099–1109.

11 A. S. Sandupatla, K. Ray, P. Thaosen, C. Sivanada and G, Deo, *Catal. Today*, 2020, **354**, 176−182.

12 E. Gomez, S. Kattel, B. Yan, S. Yao, P. Liu and J. G. Chen, Nat. *Commun*., 2018, **9**, 1398.

13 H. Wang and G. Tsilomelekis, *Catal. Sci. Technol.*, 2020, **10**, 4362−4372.

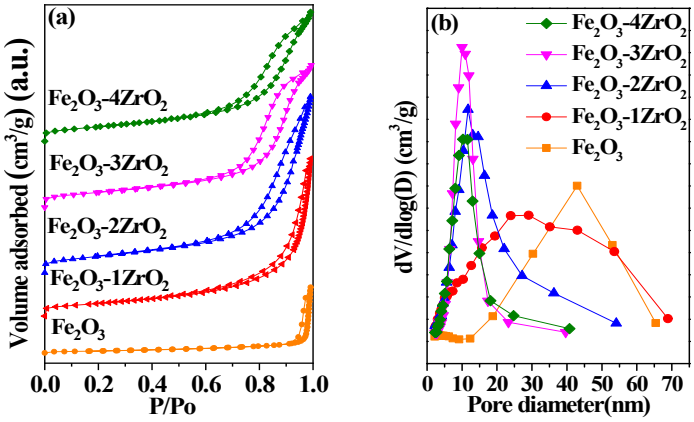

Fig. S3. N_2 adsorption-desorption isotherms (a) and pore distribution (b).

Table S2 Texture parameters of fresh catalysts

Catalysts	Specific surface area ($m^2 \cdot g^{-1}$)	Cumulative pore volume ($cm^3 \cdot g^{-1}$)	Average pore diameter(nm)
Fe_2O_3-$4ZrO_2$	56.8	0.23	11.5
Fe_2O_3-$3ZrO_2$	63.9	0.30	10.9
Fe_2O_3-$2ZrO_2$	57.4	0.29	12.6
Fe_2O_3-$1ZrO_2$	49.1	0.27	15
Fe_2O_3	8.1	0.11	29.7

Table S3 Surface element composition of fresh catalysts[a]

Catalysts	Fe (wt.%)	Zr (wt.%)	O (wt.%)	Zr/Fe (molar ratio)	Zr/Fe (nominal molar ratio)
Fe_2O_3-$4ZrO_2$	6.56	23.23	70.21	2.07	2.00
Fe_2O_3-$3ZrO_2$	8.20	22.10	69.70	1.58	1.50
Fe_2O_3-$2ZrO_2$	11.46	19.55	68.99	1.03	1.00
Fe_2O_3-$1ZrO_2$	17.34	14.59	68.07	0.52	0.50
Fe_2O_3	36.02	/	63.98	/	/

a Calculated from XPS measurement results.

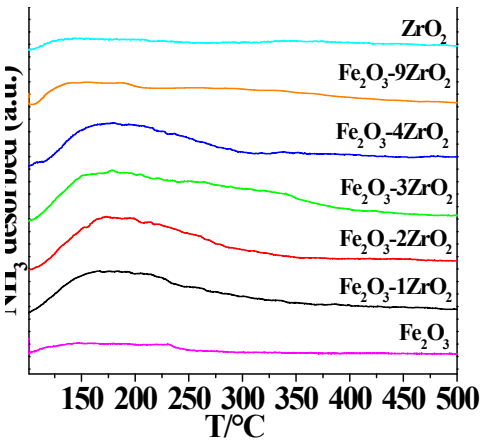

Fig. S4 NH_3-TPD profiles of fresh catalysts.

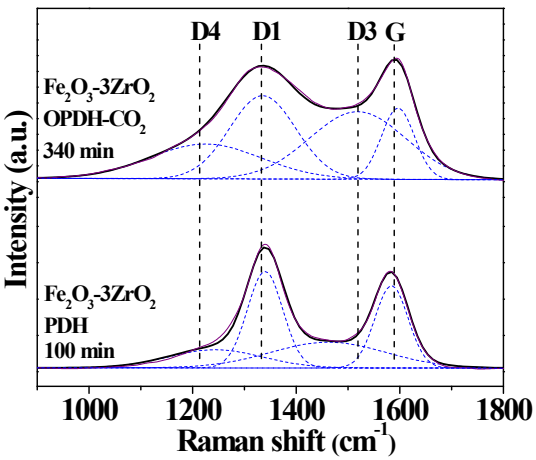

Fig. S5 Raman spectra of used catalysts.